November 2021, 64, 212201

SCIENCE CHINA
Information Sciences

• RESEARCH PAPER •

January 2021, Vol. 64 :1–:17
https://doi.org/10.1007/s11432-019-2823-9

Fixed-time attitude tracking control for spacecraft based on fixed-time extended state observer

Lijun ZHANG, Yuanqing XIA*, Ganghui SHEN & Bing CUI

School of Automation, Beijing Institute of Technology, Beijing 100081, *China*

Received 17 October 2019/Revised 31 December 2019/Accepted 5 February 2020

Abstract This paper deals with the problem of fixed-time attitude tracking control for spacecraft subject to model uncertainties and external disturbances. Firstly, by using a fixed-time extended state observer (FxTESO), the synthetic uncertainties generated by external disturbances and model deviations can be estimated and compensated accordingly. We propose a novel FxTESO aimed to improve previous methods. Unlike the existing extended state observer (ESO), the proposed FxTESO provides faster convergence and higher accuracy. Then, we design a fixed-time adaptive attitude tracking controller based on the strategy combining FxTESO and fast non-singular terminal sliding mode control (FNTSMC), such that a desired attitude can be achieved accurately, which dose not only allow providing fast and accurate responses, and acceptable chattering suppression, but also avoiding singularity. Finally, the numerical simulation results are discussed to verify the efficiency and merits of the proposed control strategy.

Keywords spacecraft, fixed time, attitude tracking, FxTESO, FNTSMC

Citation Zhang L J, Xia Y Q, Shen G H, et al. Fixed-time attitude tracking control for spacecraft based on fixed-time extended state observer. Sci China Inf Sci, 2021, 64(1): , https://doi.org/10.1007/s11432-019-2823-9

1 Introduction

Recently, attitude control of spacecraft has been attracting great attention due to its potential applications in space rendezvous and docking, spacecraft formation flying, deep space detection, and others [1–6]. Conventionally, there are the two view-points on attitude control to be considered: attitude stabilization control and attitude tracking control. The formed corresponds to the situation when the attitude of a spacecraft converges to desired constant values by applying the designed protocol [7–9]. In its turn, attitude tracking control is used to make the attitude of a spacecraft converge to desired time-variant values [10–12]. It should be noted that attitude stabilization control is a special form of attitude tracking control. Therefore, the problem of attitude tracking control corresponding to spacecraft is more widely considered among the researchers.

Moreover, this topic is important to investigate because a desired attitude can be achieved as soon as possible by applying attitude tracking control for spacecraft appropriately. Various control methods, such as optimal control [13, 14], sliding mode control (SMC) [15], adaptive control [16], and robust control [17, 18] have been discussed aiming to improve the performance of attitude tracking control. In recent years, SMC, which is insensitive to parameter uncertainties and robust against bounded external disturbances, has become one of the most widely applied control methods for spacecraft concerning the attitude tracking control problem. It is well-known that the conventional SMC may cause the chattering phenomenon. As a result, terminal SMC (TSMC) [19, 20] and fast non-singular TSMC (FNTSMC) [21] technologies have been extensively used as the enabling technology to overcome this weakness and achieve better performance compared with the traditional SMC method. It is worth mentioning that these proposed SMC extensions allow ensuring finite-time convergence. In contrast to the asymptotical convergence, finite-time convergence provides better system performance in terms of control precision, convergence rate, and robustness. However, the convergence time depends on the initial conditions of the

* Corresponding author (email: xia_yuanqing@bit.edu.cn)

system, and the initial states are usually difficult to be obtained in advance [22–24]. Therefore, applying fixed-time SMC (FxTSMC) as an attitude control approach of spacecraft is more feasible in theory and practice.

It should be noted that the existing SMC schemes cope with the uncertainties in a robust way, which means that the uncertainty attenuation ability can be achieved at the cost of its nominal control performance. During the past several years, many researchers have devoted considerable efforts to investigate and develop all kinds of observers aiming to improve the control precision under the sliding mode controller [25–31]. For instance, by utilizing SMC, the extended state observer (ESO) has been developed in [25], and the total uncertainties of the missile model have been estimated. In [26], to solve the trajectory tracking problem for a flexible joint robotic system, a feedback linearization controller based on ESO has been designed. In [27], the authors have considered the nonlinear attitude motion equations of flexible spacecraft aiming to develop a sliding mode controller using ESO. Although in [25–27] the analysis and proofs concerning ESOs have been presented, the proposed ESO has been able to ensure only the asymptotical convergence, which indicates that the uncertainties have been fully estimated as $t \to \infty$. On the basis of the SMC scheme [28], the TSMC protocol [29], FNTSMC technology [30], and high-order SMC scheme [31], the researchers have proposed four types of finite-time ESOs. However, generally, the estimation time of the existing observers is related to initial estimation errors in [28–31]. Such situation is undesirable in practical spacecraft applications, specifically, when the initial observer errors are considerably large. Therefore, it is necessary to design a novel ESO providing the fixed-time convergence to establish spacecraft attitude control appropriately. In addition, as a result of developing a well-tuned FxTESO, the estimation error is expected to be smaller than the original total uncertainties. In [15,32], the observation errors have been compensated in a robust way, which implies that the system stability can be achieved at reducing costs of the control accuracy. For this reason, it is an important challenge to develop an adaptive control strategy based on FxTESO for spacecraft, which would not only compensate the observation error, but also would converge to a small region corresponding to the tracking error in a fixed time period.

Motivated by the above discussions, the key objective of the present study is to solve the fixed-time attitude tracking problem under the designed protocols concerning the spacecraft attitude affected by model uncertainties and external disturbances. The main contributions of the present paper can be summarized as follows.

(i) The proposed FxTESO is designed to estimate the total uncertainties including the model uncertainties and external disturbances and to ensure the fixed-time convergence by using the Lyapunov method. Therefore, as a result of applying the proposed well-turned FxTESO, the estimation error is expected to be smaller compared with the original total uncertainties. (ii) A novel adaptive controller is developed by introducing the appropriately designed FxTESO and the FNTSM surface (FNTSMS) to address the attitude tracking problem for spacecraft in the fixed time.

2 Problem formulation

Let us consider the dynamic and kinematic equations corresponding to the rigid spacecraft with external disturbance as follows:

$$\begin{cases} J\dot{\omega} = -\omega^{\times} J\omega + u + z, \\ \dot{\hat{q}} = \dfrac{1}{2}(\hat{q}^{\times} + \bar{q}I_3)\omega, \quad \dot{\bar{q}} = -\dfrac{1}{2}\hat{q}^{\mathrm{T}}\omega, \end{cases} \tag{1}$$

where $J \in \mathbb{R}^{3\times 3}$, $\omega \in \mathbb{R}^3$, and $u \in \mathbb{R}^3$ represent the symmetric inertia matrix, angular velocity, and control input of the spacecraft system, respectively; $z \in \mathbb{R}^3$ denotes the unknown differentiable external disturbance. The unit quaternion $q = [\hat{q}^{\mathrm{T}},\ \bar{q}]^{\mathrm{T}} \in \mathbb{R}^4$ corresponds to the body frame of the spacecraft and is restricted to $\hat{q}^{\mathrm{T}}\hat{q} + \bar{q}^2 = 1$, where $\hat{q} = [q_1,\ q_2,\ q_3]^{\mathrm{T}} \in \mathbb{R}^3$ is the vector part and $\bar{q} \in \mathbb{R}$ is the scalar. We suppose that $q_d = [\hat{q}_d^{\mathrm{T}},\ \bar{q}_d]^{\mathrm{T}} \in \mathbb{R}^4$ can be formulated to describe a desired reference frame of the spacecraft, and then, the desired attitude motion can be modeled as follows:

$$\begin{cases} \dot{\hat{q}}_d = \dfrac{1}{2}(\hat{q}_d^{\times} + \bar{q}_d I_3)\omega_d, \\ \dot{\bar{q}}_d = -\dfrac{1}{2}\hat{q}_d^{\mathrm{T}}\omega_d, \end{cases} \tag{2}$$

where $\omega_d \in \mathbb{R}^3$ represents the desired angular velocity; ω_d and $\dot{\omega}_d$ are assumed to be bounded. The attitude tracking error $q_e = [\hat{q}_e^{\mathrm{T}},\ \bar{q}_e]^{\mathrm{T}} \in \mathbb{R}^4$ with $\hat{q}_e = [\hat{q}_{e1},\ \hat{q}_{e2},\ \hat{q}_{e3}]^{\mathrm{T}} \in \mathbb{R}^3$ denotes the relative attitude error from the body frame to the desired reference frame. The corresponding rotation matrix is defined as follows: $C(q_e) = (\bar{q}_e^2 - \hat{q}_e^{\mathrm{T}}\hat{q}_e)I_3 + 2\hat{q}_e\hat{q}_e^{\mathrm{T}} - 2\bar{q}_e\hat{q}_e^{\times}$, and the angular velocity error is denoted as $\omega_e = \omega - C(q_e)\omega_d$. Then, the attitude tracking error can be expressed as

$$\begin{cases} \hat{q}_e = \bar{q}_d\hat{q} - \hat{q}_d^{\times}\hat{q} - \bar{q}\hat{q}_d, \\ \bar{q}_e = \hat{q}_d^{\mathrm{T}}\hat{q} - \bar{q}\bar{q}_d, \end{cases} \tag{3}$$

where q_e and q_d satisfy $\|\bar{q}_e I_3 + \hat{q}_e^{\times}\| = 1$, $\|q_e\| = 1$, $\|\hat{q}_e\| \leqslant 1$, and $\|q_d\| = 1$, respectively. The corresponding tracking error system can be derived as follows:

$$\begin{cases} J\dot{\omega}_e = -(\omega_e + C(q_e)\omega_d)^{\times} J(\omega_e + C(q_e)\omega_d) + J(\omega_e^{\times}C(q_e)\omega_d - C(q_e)\dot{\omega}_d) + u + z, \\ \dot{\hat{q}}_e = \dfrac{1}{2}\sigma(q_e)\omega_e, \quad \dot{\bar{q}}_e = -\dfrac{1}{2}\hat{q}_e^{\mathrm{T}}\omega_e, \end{cases} \tag{4}$$

where $\sigma(q_e) = \hat{q}_e^{\times} + \bar{q}_e I_3$.

The key objective of the present study is to address the attitude and angular velocity tracking problem of spacecraft affected by model uncertainties and external disturbances under a fixed-time adaptive controller, such that the attitude and angular velocity tracking errors would converge to small region around the origin, respectively.

Before providing the main results, the following assumptions and lemmas are formulated to facilitate development of the fixed-time attitude tracking controller for spacecraft under consideration.

Assumption 1. Let the inertia matrix $J = J_0 + \Delta J$, with J_0 be a known nonsingular constant matrix, and ΔJ be an uncertainty matrix.

Assumption 2. The disturbance d is assumed to be bounded as follows: $|d_i| \leqslant d_0$ $(i = 1, 2, 3)$, where $d_0 > 0$ is an unknown positive constant.

Lemma 1 ([33])**.** For $x_i \in \mathbb{R}$, $i = 1, 2, \ldots, n$, $0 < h \leqslant 1$, then $(\sum_{i=1}^n x_i)^h \leqslant \sum_{i=1}^n |x_i|^h \leqslant n^{1-h}(\sum_{i=1}^n x_i)^h$. $h > 1$, then $\sum_{i=1}^n |x_i|^h \leqslant (\sum_{i=1}^n x_i)^h \leqslant n^{h-1}\sum_{i=1}^n |x_i|^h$.

Lemma 2 ([34])**.** For $\tilde{x} \in \mathbb{R}$, $\hat{x} \in \mathbb{R}$, the following statements hold: $x \in \mathbb{R}$ and $h > \frac{1}{2}$. Let us define $x = \tilde{x} + \hat{x}$, then, the following inequality can be formulated: $\tilde{x}\hat{x} = -\tilde{x}^2 + x\tilde{x} \leqslant \frac{h}{2}x^2 + \frac{\tilde{x}^2}{2h} - \tilde{x}^2 \leqslant -\frac{2h-1}{2h}\tilde{x}^2 + \frac{h}{2}x^2$.

Lemma 3 ([35])**.** If an $n \times n$ matrix P is real symmetric positive definite, then

$$\lambda_{\min}(P)\|x\|^2 \leqslant x^{\mathrm{T}}Px \leqslant \lambda_{\max}(P)\|x\|^2,$$

where $\lambda_{\min}(P)$ and $\lambda_{\max}(P)$ are the minimum and maximum eigenvalues of a matrix P, respectively.

Lemma 4 ([36])**.** Let us suppose that V_1 and V_2 are the continuous real-valued functions on $\mathbb{R}^n$, homogeneous with respect to ν of degrees $l_1 > 0$ and $l_2 > 0$, respectively, and V_1 is positive definite. Then, for every $x \in \mathbb{R}^n$:

$$\big[\min_{z:V_1(z)=1} V_2(z)\big][V_1(x)]^{\frac{l_2}{l_1}} \leqslant V_2(x) \leqslant \big[\max_{z:V_1(z)=1} V_2(z)\big][V_1(x)]^{\frac{l_2}{l_1}}.$$

Lemma 5 ([37,38])**.** Let us consider the following nonlinear system formulated as follows:

$$\dot{x} = f(x,t), \quad f(0,t) = 0, \quad x \in U \subset \mathbb{R}^n, \tag{5}$$

where $f : U \times \mathbb{R}^+ \to \mathbb{R}^n$ is continuous on an open neighborhood U of the origin $x = 0$. The zero solution of (5) is finite-time stable if it is Lyapunov stable and finite-time convergent in a neighborhood $U_0 \subseteq U$ of the origin. Let us suppose that there is a Lyapunov function $V(x,t)$ defined on $U_1 \times \mathbb{R}^+$, where $U_1 \subseteq U \in \mathbb{R}^n$ in a neighborhood of the origin.

If there exist any real numbers $\lambda > 0$ and $0 < \alpha < 1$, and $U_1 \subseteq U$ of the origin such that

$$\dot{V}(x,t) + \lambda V^{\alpha}(x,t) \leqslant 0, \quad x \in U_1 \setminus \{0\},$$

then, the origin of system (5) is considered as locally finite-time stable, and the settling-time is estimated as follows:

$$T_r \leqslant \frac{V^{1-\alpha}(x_0)}{\lambda_2(1-\alpha)},$$

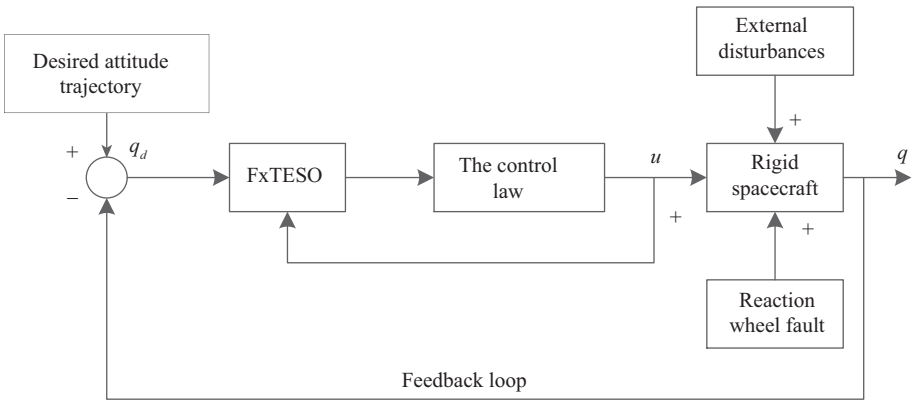

Figure 1 The fixed-time attitude tracking control structure.

where $V(x_0)$ is the initial value of $V(x,t)$.

If there exist positive parameters $\alpha,\ \beta,\ p,\ q,\ k,\ pk<1,\ qk>1$, and $0<\delta<\infty$, such that

$$\dot{V}(x,t)\leqslant -(\alpha V^p(x(x,t))+\beta V^q(x(x,t)))^k+\delta,$$

then, the origin of system (5) is practical fixed-time stable, and the settling time indicates that $T(x_0)\leqslant \frac{1}{\alpha^k(1-pk)}+\frac{1}{\beta^k(qk-1)},\ \forall x_0\in\mathbb{R}^n$.

3 Attitude tracking control

In this section, we discuss the FNTSMC controller design for spacecraft subject to model uncertainties and external disturbances. Figure 1 represents the fixed-time attitude tracking control structure, which is composed of the FNTSMS (6), FxTESO (20), and the adaptive controllers (33)–(35). Subsection 3.1 outlines the details about FNTSMS constructed to ensure the tracking performance. Subsection 3.2 provides the description of the proposed FxTESO design aimed to designed to estimate and compensate the uncertainties generated by model uncertainties and external disturbances. Subsection 3.3 provides the discussion on the adaptive control strategy designed to ensure that the closed-loop system based on the FNTSMS (6) and FxTESO (20) is fixed-time stable.

3.1 Sliding mode surface design

In this subsection, the design of FNTSMS is described as follows:

$$S=\omega_e+2k_1\sigma^{-1}(q_e)\mathrm{sig}^{r_1}(\hat{q}_e)+2k_2\sigma^{-1}(q_e)S_{\mathrm{au}},\tag{6}$$

where $S=[S_1,\ S_2,\ S_3]^{\mathrm{T}}\in\mathbb{R}^3$; $\mathrm{sign}(\cdot)$ denotes the sign function; $\mathrm{sig}^{\bar{\alpha}}(x)=|x|^{\bar{\alpha}}\mathrm{sign}(x)$ with $\bar{\alpha}>0$; $r_1=\frac{r_{11}}{r_{12}}>1$, $0<r_2=\frac{r_{21}}{r_{22}}<1$, $r_{11},\ r_{12}$, r_{21}, and r_{22} are positive odd numbers; and $k_1>0$, $k_2>0$. Let us denote $S_{\mathrm{au}}=[S_{\mathrm{au1}},\ S_{\mathrm{au2}},\ S_{\mathrm{au3}}]^{\mathrm{T}}$, and then, $S_{\mathrm{au}i}$ is designed as follows:

$$S_{\mathrm{au}i}=\begin{cases}\mathrm{sig}^{r_2}(\hat{q}_{ei}), & \text{if } \bar{S}_i=0 \text{ or } \bar{S}_i\neq 0,\ |\hat{q}_{ei}|\geqslant\phi,\\ \iota_1\hat{q}_{ei}+\iota_2\mathrm{sig}^2(\hat{q}_{ei}), & \text{if } \bar{S}_i\neq 0,\ |\hat{q}_{ei}|<\phi,\end{cases}\tag{7}$$

where $\bar{S}=\omega_e+2k_1\sigma^{-1}(q_e)\mathrm{sig}^{r_1}(\hat{q}_e)+2k_2\sigma^{-1}(q_e)\mathrm{sig}^{r_2}(\hat{q}_e)$; $\iota_1=(2-r_2)\phi^{r_2-1}$; $\iota_2=(r_2-1)\phi^{r_2-2}$; and $\phi>0$.

Lemma 6. Considering the attitude tracking error system (4) based on FNTSMS (6), let us assume that there exists $S=\bar{S}=0$, such that $\{\bar{q}_e(t)\equiv 1,\ \omega_e(t)\equiv\mathbf{0}\}$ can be achieved in fixed time T_0. Then, the fixed time T_0 is expressed as follows:

$$T_0\leqslant\frac{2}{(1+r_1)\alpha}+\frac{2}{(1+r_2)\beta}.\tag{8}$$

Proof. If FNTSMS $S_i = \bar{S}_i = 0$, we obtain

$$\omega_e = -2k_1\sigma^{-1}(q_e)\mathrm{sig}^{r_1}(\hat{q}_e) - 2k_2\sigma^{-1}(q_e)\mathrm{sig}^{r_2}(\hat{q}_e). \tag{9}$$

Due to (4), the $\dot{\hat{q}}_e$ can further be expressed as follows:

$$\dot{\hat{q}}_e = -k_1\mathrm{sig}^{r_1}(\hat{q}_e) - k_2\mathrm{sig}^{r_2}(\hat{q}_e). \tag{10}$$

Let us construct the Lyapunov function as follows:

$$V_0 = \frac{1}{2}\hat{q}_e^{\mathrm{T}}\hat{q}_e. \tag{11}$$

Taking the derivative of V_0, we can yield that

$$\begin{aligned}\dot{V}_0 &= \hat{q}_e^{\mathrm{T}}\dot{\hat{q}}_e = \hat{q}_e^{\mathrm{T}}(-k_1\mathrm{sig}^{r_1}(\hat{q}_e) - k_2\mathrm{sig}^{r_2}(\hat{q}_e)) \\ &\leqslant -k_1\sum_{i=1}^{3}(\hat{q}_{ei}^2)^{\frac{1+r_1}{2}} - k_2\sum_{i=1}^{3}(\hat{q}_{ei}^2)^{\frac{1+r_2}{2}}.\end{aligned} \tag{12}$$

Based on Lemma 1, it is possible to obtain that

$$\sum_{i=1}^{3}(\hat{q}_{ei}^2)^{\frac{1+r_1}{2}} \geqslant 3^{\frac{1-r_1}{2}}\left(\sum_{i=1}^{3}\hat{q}_{ei}^2\right)^{\frac{1+r_1}{2}},$$

and

$$\sum_{i=1}^{3}(\hat{q}_{ei}^2)^{\frac{1+r_2}{2}} \geqslant \left(\sum_{i=1}^{3}\hat{q}_{ei}^2\right)^{\frac{1+r_2}{2}}.$$

Then, we formulate the following

$$\begin{aligned}\dot{V}_0 &\leqslant -k_1 3^{\frac{1-r_1}{2}}\left(\sum_{i=1}^{3}\hat{q}_{ei}^2\right)^{\frac{1+r_1}{2}} - k_2\left(\sum_{i=1}^{3}\hat{q}_{ei}^2\right)^{\frac{1+r_2}{2}} \\ &\leqslant -\alpha V_0^{\frac{1+r_1}{2}} - \beta V_0^{\frac{1+r_2}{2}},\end{aligned} \tag{13}$$

where $\alpha = 2^{\frac{1+r_1}{2}}3^{\frac{1-r_1}{2}}k_1$, and $\beta = 2^{\frac{1+r_2}{2}}k_2$. By considering Lemma 5, it can be observed that $\lim_{t\to T_0}\hat{q}_e(t) = \mathbf{0}$, and $\lim_{t\to T_0}\omega_e(t) = \mathbf{0}$ in the fixed time. Furthermore, we can obtain that $\lim_{t\to T_0}\bar{q}_e(t) = 1$ or -1.

Considering the scenario of $(\bar{q}_e, \hat{q}_e) = (-1, \mathbf{0})$, we show that $(\bar{q}_e, \hat{q}_e) = (-1, \mathbf{0})$ is not a stable equilibrium point in the reaching phase. Let us construct the following function as

$$V_{01} = \hat{q}_e^{\mathrm{T}}\hat{q}_e + (1 + \bar{q}_e)^2. \tag{14}$$

Through the simple computation, we obtain that

$$\begin{aligned}\dot{V}_{01} &= 2\hat{q}_e^{\mathrm{T}}\dot{\hat{q}}_e + 2(1 + \bar{q}_e)\dot{\bar{q}}_e \\ &= \hat{q}_e^{\mathrm{T}}(\hat{q}_e^{\times} + \bar{q}_e I_3)\omega_e - (1 + \bar{q}_e)\hat{q}_e^{\mathrm{T}}\omega_e \\ &= -\hat{q}_e^{\mathrm{T}}\omega_e \\ &= \hat{q}_e^{\mathrm{T}}\left(2k_1\sigma^{-1}\mathrm{sig}^{r_1}(q_e)(\hat{q}_e) + 2k_2\sigma^{-1}(q_e)\mathrm{sig}^{r_2}(\hat{q}_e)\right) \\ &\leqslant 3^{\frac{1-r_1}{2}}2k_1\left(\sum_{i=1}^{3}\hat{q}_{ei}^2\right)^{\frac{1+r_1}{2}} + 2k_2\left(\sum_{i=1}^{3}\hat{q}_{ei}^2\right)^{\frac{1+r_2}{2}}.\end{aligned} \tag{15}$$

According to the Lyapunov instability theorem described in [39], it can be seen that $(\bar{q}_e, \hat{q}_e) = (-1, \mathbf{0})$ is not a stable equilibrium point, and therefore, we select $(\bar{q}_e, \hat{q}_e) = (1, \mathbf{0})$ as an equilibrium point.

It should be noted that $r_1 > 1$, and $0 < r_2 < 1$; so that $\frac{1+r_1}{2} > 1$, and $\frac{1}{2} < \frac{1+r_2}{2} < 1$. By considering Lemma 5, the objective $\{\hat{q}_e(t) \equiv \mathbf{0},\ \bar{q}_e(t) \equiv 1,\ \omega_e(t) \equiv \mathbf{0}\}$ can be guaranteed in fixed time T_0.

Referring to Assumption 1, we can obtain the following:

$$\begin{aligned} J_0\dot{S} =& (J-\Delta J)\big(\dot{\omega}_e + 2r_1k_1\sigma^{-1}(q_e)\mathrm{diag}\{|\hat{q}_{ei}|^{r_1-1}\}\dot{\hat{q}}_e + 2k_2\sigma^{-1}(q_e)\dot{S}_{\mathrm{au}} + 2k_1\dot{\sigma}^{-1}\hat{q}_e^{r_1} + 2k_2\dot{\sigma}^{-1}S_{\mathrm{au}}\big) \\ =& -(\omega_e + C(q_e)\omega_d)^{\times}(J_0+\Delta J)(\omega_e + C(q_e)\omega_d) + (J_0+\Delta J)(\omega_e^{\times}C(q_e)\omega_d - C(q_e)\dot{\omega}_d) + u + d - \Delta J\dot{\omega}_e \\ &+ r_1k_1J_0\sigma^{-1}\mathrm{diag}\{|\hat{q}_{ei}|^{r_1-1}\}\sigma\omega_e + k_2J_0\sigma^{-1}E_{\mathrm{au}}\sigma\omega_e + 2k_1J_0\dot{\sigma}^{-1}\mathrm{sig}^{r_1}(\hat{q}_e) + 2k_2J_0\dot{\sigma}^{-1}S_{\mathrm{au}}, \end{aligned} \tag{16}$$

where

$$E_{\mathrm{au}i} = \begin{cases} r_2|\hat{q}_{ei}|^{r_2-1}, & \text{if } \bar{S}_i = 0 \text{ or } \bar{S}_i \neq 0,\ |\hat{q}_{ei}| \geqslant \phi, \\ \iota_1 + 2\iota_2|\hat{q}_{ei}|, & \text{if } \bar{S}_i \neq 0,\ |\hat{q}_{ei}| < \phi. \end{cases}$$

Consequently, Eq. (16) can be rewritten as follows:

$$J_0\dot{S} = F + G + u, \tag{17}$$

where

$$\begin{aligned} F =& -(\omega_e + C(q_e)\omega_d)^{\times}J_0(\omega_e + C(q_e)\omega_d) + J_0(\omega_e^{\times}C(q_e)\omega_d - C(q_e)\dot{\omega}_d) + r_1k_1J_0\sigma^{-1}\mathrm{diag}\{|\hat{q}_{ei}|^{r_1-1}\}\sigma\omega_e \\ &+ k_2J_0\sigma^{-1}E_{\mathrm{au}}\sigma\omega_e + 2k_1J_0\dot{\sigma}^{-1}\hat{q}_e^{r_1} + 2k_2J_0\dot{\sigma}^{-1}S_{\mathrm{au}}, \\ G =& -(\omega_e + C(q_e)\omega_d)^{\times}\Delta J(\omega_e + C(q_e)\omega_d) + \Delta J(\omega_e^{\times}C(q_e)\omega_d - C(q_e)\dot{\omega}_d) + z - \Delta J\dot{\omega}_e \\ =& (I_3 - \Delta JJ^{-1})z - \omega^{\times}\Delta J\omega + \Delta JJ^{-1}\omega^{\times}J\omega + \Delta JJ^{-1}u. \end{aligned} \tag{18}$$

3.2 Fixed-time extended state observer design

In this subsection, we describe the design of FxTESO proposed to estimate and compensate the synthetic uncertainties in the fixed time. Let us define coordinate transformation as $J_0S = x_1$. The extended state x_2, which is considered instead of the total uncertainty G, is added. We denote $g = \dot{x}_2$, and $\|g\| \leqslant \bar{g}$ with $\bar{g}$ being a positive constant. The system model (17) can be further represented as follows:

$$\begin{cases} \dot{x}_1 = F + x_2 + u, \\ \dot{x}_2 = g(t), \end{cases} \tag{19}$$

where $g(t) = [g_1(t),\ g_2(t),\ g_3(t)]^{\mathrm{T}}$. Then, the second-order FxTESO is proposed as follows:

$$\begin{cases} \dot{Z}_1 = F + Z_2 + u + \alpha_1\Lambda\mathrm{sig}^{o_1}(x_1 - Z_1) + \beta_1(1-\Lambda)\mathrm{sig}^{\theta_1}(x_1 - Z_1), \\ \dot{Z}_2 = \alpha_2\Lambda\mathrm{sig}^{o_2}(x_1 - Z_1) + \beta_2(1-\Lambda)\mathrm{sig}^{\theta_2}(x_1 - Z_1) + \gamma\mathrm{sign}(x_1 - Z_1), \end{cases} \tag{20}$$

where Z_1 and Z_2 approach J_0S and G, respectively. $\alpha_1,\ \alpha_2,\ \beta_1,\ \beta_2$, and γ are the observer gains, with $\gamma > \bar{g}$. Here, $o_1 = o \in (1-\varepsilon, 1)$; $\theta_1 = \theta \in (1, 1+\varepsilon)$; $o_2 = 2o - 1$; $\theta_2 = 2\theta - 1$; and ε is a sufficiently small number. The indicator function Λ satisfies the following rule:

$$\Lambda = \begin{cases} 0, & \text{if } t \leqslant T^*, \\ 1, & \text{if } t > T^*, \end{cases} \tag{21}$$

where T^* is the switching time, which depends on the observation error.

Let us define $E_1 = x_1 - Z_1$, and $E_2 = x_2 - Z_2$. Then, it follows that the observation error dynamics can be rewritten as follows:

$$\begin{cases} \dot{E}_1 = E_2 - \alpha_1\Lambda\mathrm{sig}^{o_1}(E_1) - \beta_1(1-\Lambda)\mathrm{sig}^{\theta_1}(E_1), \\ \dot{E}_2 = -\big(\alpha_2\Lambda\mathrm{sig}^{o_2}(E_1) + \beta_2(1-\Lambda)\mathrm{sig}^{\theta_2}(E_1) + \gamma\mathrm{sign}(E_1)\big) + g(t). \end{cases} \tag{22}$$

Theorem 1. Let us consider the spacecraft system (4) based on FxTESO (20). There exist the appropriate observation gains $\alpha_1,\ \alpha_2,\ \beta_1,\ \beta_2$, and $0 < o < 1$, $\theta > 1$, such that E_1 converges to zero in fixed time T_1 without the initial conditions for $t > T_1$, and the observation error E_2 converges to a small region

ε_1 within the fixed time $t < T_c = T_1 + T_2$. Then, the expressions of the convergence time can be defined as follows:

$$\begin{aligned} T_1 &\leqslant \frac{\lambda_{\max}(P)}{\lambda_{\min}(Q)} \frac{2}{1-o} \left(\frac{\theta-1}{2} \frac{2\lambda_{\min}(Q)}{\lambda_{\max}(P) T^*} \right)^{\frac{1-o}{1-\theta}} + T^*, \\ T_2 &\leqslant \frac{\varepsilon_1}{\gamma - \bar{g}}, \end{aligned} \tag{23}$$

where ε_1 is a sufficiently small parameter.

Proof. Let us define $\epsilon = [[\mathrm{sig}(E_1)]^{\mathrm{T}},\ [\mathrm{sig}^{\frac{1}{\theta}}(E_2)]^{\mathrm{T}}]^{\mathrm{T}}$, and $E = [E_1^{\mathrm{T}},\ E_2^{\mathrm{T}}]^{\mathrm{T}}$. With respect to (21), $\Lambda = 0$ if $t \leqslant T^*$. Then, the error estimation equation (22) can be rewritten as follows:

$$\begin{cases} \dot{E}_1 = E_2 - \beta_1 \mathrm{sig}^{\theta_1}(E_1), \\ \dot{E}_2 = -\beta_2 \mathrm{sig}^{\theta_2}(E_1). \end{cases} \tag{24}$$

Let us define $A \in \mathbb{R}^{6\times 6}$ as follows:

$$A = \begin{bmatrix} -\beta_1 I_3 & I_3 \\ -\beta_2 I_3 & 0 \end{bmatrix}.$$

Then, there exists $P = P^{\mathrm{T}} > 0$, such that $A^{\mathrm{T}}P + PA = -Q$, and A is a Hurwitz matrix.

Let us construct the Lyapunov function candidate as follows:

$$V_1(\theta, \epsilon) = \epsilon^{\mathrm{T}} P \epsilon. \tag{25}$$

It holds that the observation errors E_1 and E_2 are asymptotically stable for $\theta = 1$; namely, $\dot{E} = AE$. Taking the derivative of $V_1(1, \epsilon)$, we can yield the following:

$$\dot{V}_1(1, \epsilon) = \dot{\epsilon}^{\mathrm{T}} P \epsilon + \epsilon^{\mathrm{T}} P \dot{\epsilon} = E^{\mathrm{T}}(A^{\mathrm{T}}P + PA)E = -E^{\mathrm{T}} Q E \leqslant 0. \tag{26}$$

By applying Lemma 3 and (25), we obtain the following:

$$V_1(1, \epsilon) \leqslant \lambda_{\max}(P) \|\epsilon\|^2,$$

and

$$\dot{V}_1(1, \epsilon) \leqslant -\lambda_{\min}(Q) \|\epsilon\|^2.$$

Therefore, it is possible to obtain that

$$\dot{V}_1(1, \epsilon) \leqslant -c V_1(1, \epsilon), \tag{27}$$

where $c = \frac{\lambda_{\min}(Q)}{\lambda_{\max}(P)}$.

From the inequality $\dot{V}_1(1, \epsilon) < 0$, it can be seen that $\dot{V}_1(\theta, \epsilon) < 0$ also holds, as noted in [40], implying that the system (24) is asymptotically stable.

Moreover, it is possible to verify that the system (24) is homogeneous of degree $\theta - 1$ with respect to weights 1 and θ. Let f be the vector field of (24) that is homogeneous of degree 2. Therefore, according to Lemma 4, the following inequality holds:

$$\dot{V}_1(\theta, \epsilon) \leqslant -c V_1^{\frac{1+\theta}{2}}(\theta, \epsilon).$$

When $t = T^*$, the following condition for $V_1(\theta, \epsilon)$ is satisfied

$$\begin{aligned} V_1(\theta, \epsilon) &\leqslant \left(\frac{\theta-1}{2} \frac{\lambda_{\min}(Q)}{\lambda_{\max}(P)} T^* + (V_1(\theta, \epsilon)|_0)^{\frac{1-\theta}{2}} \right)^{\frac{2}{1-\theta}} \\ &\leqslant \left(\frac{\theta-1}{2} \frac{\lambda_{\min}(Q)}{\lambda_{\max}(P)} T^* \right)^{\frac{2}{1-\theta}}. \end{aligned} \tag{28}$$

$\Lambda = 1$, if $t > T^*$. The observation error system (22) can be rewritten as follows:

$$\begin{cases} \dot{E}_1 = E_2 - \alpha_1 \mathrm{sig}^{o_1}(E_1), \\ \dot{E}_2 = -\alpha_2 \mathrm{sig}^{o_2}(E_1). \end{cases} \tag{29}$$

Similarly, we construct another Lyapunov function as follows: $V_2(o, \bar{\epsilon}) = \bar{\epsilon}^{\mathrm{T}} P \bar{\epsilon}$, where $\bar{\epsilon} = [[\mathrm{sig}(E_1)]^{\mathrm{T}}, [\mathrm{sig}^{\frac{1}{o}}(E_2)]^{\mathrm{T}}]^{\mathrm{T}}$. It is possible to obtain that

$$\dot{V}_2(o, \bar{\epsilon}) \leqslant -c V_2^{\frac{1+o}{2}}(o, \bar{\epsilon}). \tag{30}$$

As $o \in (1 - \varepsilon, 1)$, we note that $V_1(\theta, \epsilon)|_{T^*}$ is the initial condition of $V_2(o, \bar{\epsilon})$. We observe that the observation error converges to zero within fixed time T_1 by applying Lemma 5 to (30), implying that $E_1 = \dot{E}_1 = 0$, for all $t \geqslant T_1$. Then, the following equation defined in (22) can be further rewritten as follows:

$$\dot{E}_{2i} = g_i - \gamma \mathrm{sign}(E_{1i}). \tag{31}$$

It can be seen that if $E_{2i} \to \varepsilon_1$, the above equation can be written as follows:

$$\dot{E}_{2i} = g_i - \gamma \mathrm{sign}(E_{1i}) = 0, \text{ for } t \geqslant T_1. \tag{32}$$

Selecting a sufficiently small parameter ε_1, we obtain that if $(E_{1i})_{eq} > 0$, then $\dot{E}_{2i} \leqslant \bar{g} - \gamma$, and if $(E_{1i})_{eq} < 0$, then $-\dot{E}_{2i} \geqslant \gamma - \bar{g}$. Then, the observation error $|E_{2i}|$ converges to a small region ε_1 in fixed time T_2.

Remark 1. It should be noted that the proposed FxTESO can provide a faster convergence rate compared with the observer suggested in [25, 41, 42]. The term $\beta_1(1 - \Lambda)\mathrm{sig}^{\theta_1}(x_1 - Z_1)$ can be used to improve the convergence performance owing to the application of a switching signal $\Lambda = 0$, when the estimation errors are far away from the equilibrium. The term $\alpha_1 \Lambda \mathrm{sig}^{o_1}(x_1 - Z_1)$ plays a major role during the application of a switching signal $\Lambda = 1$, when the estimation errors are near the equilibrium. Moreover, the upper bound of the estimation time is independent of the initial estimation errors. This means that the estimation time can be obtained in a more convenient manner by tuning the observer gains.

3.3 Adaptive controller design

Based on FNTSMS, FxTESO, and the previous analysis, we propose the following desired controller:

$$u = -(k_3 \mathrm{sig}^{r_3}(S) + k_4 \mathrm{sig}^{r_4}(S) + k_5 S + Z_2 + F + u_{\mathrm{adp}}), \tag{33}$$

where $k_3 > 0$, $k_4 > 0$, $k_5 > 0$, $r_3 > 1$, and $0 < r_4 < 1$. Let us denote $u_{\mathrm{adp}} = [u_{\mathrm{adp1}},\ u_{\mathrm{adp2}},\ u_{\mathrm{adp3}}]^{\mathrm{T}}$, where $u_{\mathrm{adp}i}$ is designed as follows:

$$u_{\mathrm{adp}i} = \begin{cases} \dfrac{S_i}{|S_i|}\hat{\varepsilon}_1, & \text{if } |S_i| \geqslant \varepsilon_0, \\ \dfrac{S_i}{\varepsilon_0^2}\hat{\varepsilon}_1^2, & \text{if } |S_i| < \varepsilon_0. \end{cases} \tag{34}$$

The adaption update law is defined as follows:

$$\dot{\hat{\varepsilon}}_1 = k_0(\|S\| - k_6 \hat{\varepsilon}_1), \tag{35}$$

where k_0 and k_6 are constants; $\hat{\varepsilon}_1$ is the estimation of ε_1; and $\tilde{\varepsilon}_1 = \varepsilon_1 - \hat{\varepsilon}_1$.

Remark 2. Considering the recent results on the ESO-based sliding mode finite-time attitude tracking control for spacecraft [28–31], it has been shown that the unknown signal cannot be tracked completely by the observer. It has been also shown that the convergence region is affected by the observation error of the extended state observer. Therefore, an adaptive law is designed to compensate for the observation error with the purpose not only to assure the tracking disturbance performance of the observer, but also to guarantee the convergence performance to the sliding mode surface.

Theorem 2. Considering the spacecraft system (19) using FNTSMS (6) and FxTESO (20), the trajectory of the sliding surface S converges into Δ_S in fixed time $t \leqslant T_r = T_1 + T_2 + T_3$ under the controller (33) and the adaptive law (35). Furthermore, the attitude tracking errors $\hat{q}_{ei}$ $(i = 1, 2, 3)$ converge to region Δ_1 in the fixed time, and the angular velocity errors ω_{ei} $(i = 1, 2, 3)$ converge to region Δ_2 in the fixed time. The expressions of the convergence regions are defined as follows:

$$\Delta_S = \max(\Delta_{S1}, \Delta_{S2}), \tag{36}$$

$$\Delta_{S1} = \min\left(\sqrt{\frac{2}{\lambda_{\max}(J_0)}}\left(\frac{\eta}{\tau_1}\right)^{\frac{1}{1+r_3}}, \sqrt{\frac{2}{\lambda_{\max}(J_0)}}\left(\frac{\eta}{\tau_2}\right)^{\frac{1}{1+r_4}}\right),$$

$$\Delta_{S2} = \min\left(\varepsilon_0, \frac{\chi}{k_5}\right),$$

$$\Delta_1 = \max(\phi, \phi_1), \quad \phi_1 = \min\left(\sqrt[r_1]{\frac{\Delta_S}{k_1}}, \sqrt[r_2]{\frac{\Delta_S}{k_2}}\right), \tag{37}$$

$$\Delta_2 = \Delta_S + k_1\Delta_1^{r_1} + k_2\Delta_1^{r_2}, \tag{38}$$

and the fixed time T_3 can be calculated as follows:

$$T_3 \leqslant \frac{2}{\tau_2(r_3 - 1)} + \frac{2}{\tau_1(1 - r_4)}, \tag{39}$$

where $\tau_1 = 3^{\frac{1-r_3}{2}}(\frac{2}{\lambda_{\max}(J_0)})^{\frac{1+r_3}{2}}k_3$ and $\tau_2 = (\frac{2}{\lambda_{\max}(J_0)})^{\frac{1+r_4}{2}}k_4$.

Proof. The proof of the result can be performed according to the following two steps.

Step 1. In this step, we prove that the sliding variable S can converge to Δ_S in the fixed time. The Lyapunov function can be formulated as follows:

$$V_3 = \frac{1}{2}S^{\mathrm{T}}J_0S + \frac{1}{2k_0}\tilde{\varepsilon}_1^2. \tag{40}$$

Taking the derivative of V_3, we can yield that

$$\begin{aligned}\dot{V}_3 &= S^{\mathrm{T}}(F + x_2 + u) - \frac{1}{k_0}\tilde{\varepsilon}_1\dot{\hat{\varepsilon}}_1 \\ &= S^{\mathrm{T}}(-k_3\mathrm{sig}^{r_3}(S) - k_4\mathrm{sig}^{r_4}(S) - k_5S - Z_2 + x_2 - u_{\mathrm{adp}}) - \frac{1}{k_0}\tilde{\varepsilon}_1\dot{\hat{\varepsilon}}_1.\end{aligned} \tag{41}$$

For the case of $|S_i| < \varepsilon_0$, substituting the (34) into (41) yields the following:

$$\begin{aligned}\dot{V}_3 \leqslant& -k_3S^{\mathrm{T}}\mathrm{sig}^{r_3}(S) - k_4S^{\mathrm{T}}\mathrm{sig}^{r_4}(S) - k_5S^{\mathrm{T}}S + \|S\|\|E\| - \left[\left(\frac{\|S\|}{\varepsilon_0}\hat{\varepsilon}_1 - \frac{\varepsilon_0}{2}\right)^2 + \|S\|\hat{\varepsilon}_1 - \frac{\varepsilon_0^2}{4}\right] \\ &- \|S\|\tilde{\varepsilon}_1 + k_6\tilde{\varepsilon}_1\hat{\varepsilon}_1 \\ \leqslant& -k_3S^{\mathrm{T}}\mathrm{sig}^{r_3}(S) - k_4S^{\mathrm{T}}\mathrm{sig}^{r_4}(S) - k_5S^{\mathrm{T}}S - \left(\frac{\|S\|}{\varepsilon_0}\hat{\varepsilon}_1 - \frac{\varepsilon_0}{2}\right)^2 + \frac{\varepsilon_0^2}{4} + k_6\tilde{\varepsilon}_1\hat{\varepsilon}_1.\end{aligned} \tag{42}$$

Considering Lemma 2, we can obtain that

$$\tilde{\varepsilon}_1\hat{\varepsilon}_1 \leqslant -\frac{2\lambda - 1}{2\lambda}\tilde{\varepsilon}_1^2 + \frac{\lambda}{2}\varepsilon_1^2.$$

Eq. (42) can be rewritten as follows:

$$\dot{V}_3 \leqslant -k_3S^{\mathrm{T}}\mathrm{sig}^{r_3}(S) - k_4S^{\mathrm{T}}\mathrm{sig}^{r_4}(S) + \frac{\varepsilon_0^2}{4} + \frac{\lambda k_6}{2}\varepsilon_1^2$$

$$\leqslant -\tau_1 V_3^{\frac{1+r_3}{2}} - \tau_2 V_3^{\frac{1+r_4}{2}} + \eta, \tag{43}$$

where $\eta = \frac{\varepsilon_0^2}{4} + \frac{\lambda k_6}{2}\varepsilon_1^2$, $\tau_1 = 3^{\frac{1-r_3}{2}}(\frac{2}{\lambda_{\max}(J_0)})^{\frac{1+r_3}{2}}k_3$, and $\tau_2 = (\frac{2}{\lambda_{\max}(J_0)})^{\frac{1+r_4}{2}}k_4$.

According to Lemma 5, we conclude that FNTSMS converges to the region Δ_{S1} when $|S_i| < \varepsilon_0$.

For the case of $|S_i| \geqslant \varepsilon_0$, Eq. (41) can be rewritten as follows:

$$\begin{aligned}\dot{V}_3 \leqslant & -k_3 S^{\mathrm{T}}\mathrm{sig}^{r_3}(S) - k_4 S^{\mathrm{T}}\mathrm{sig}^{r_4}(S) - k_5 S^{\mathrm{T}}S + \|S\|\|E_2\| - \|S\|\hat{\varepsilon}_1 - \tilde{\varepsilon}_1\|S\| + k_6\tilde{\varepsilon}_1\hat{\varepsilon}_1 \\ \leqslant & -k_3 S^{\mathrm{T}}\mathrm{sig}^{r_3}(S) - k_4 S^{\mathrm{T}}\mathrm{sig}^{r_4}(S) - k_5 S^{\mathrm{T}}S + k_6\tilde{\varepsilon}_1\hat{\varepsilon}_1 \\ \leqslant & -k_3 S^{\mathrm{T}}\mathrm{sig}^{r_3}(S) - k_4 S^{\mathrm{T}}\mathrm{sig}^{r_4}(S) - k_5 S^{\mathrm{T}}S - \frac{k_6(2\lambda-1)}{2\lambda}\tilde{\varepsilon}_1^2 + \frac{\lambda k_6}{2}\varepsilon_1^2.\end{aligned} \tag{44}$$

Therefore, the trajectories of S, $\tilde{\varepsilon}_1$ are bounded when $|S_i| \geqslant \varepsilon_0$.

We construct the Lyapunov function as: $V_4 = \frac{1}{2}S^{\mathrm{T}}J_0 S$. Differentiating V_4 yields the following:

$$\begin{aligned}\dot{V}_4 \leqslant & -k_3 S^{\mathrm{T}}\mathrm{sig}^{r_3}(S) - k_4 S^{\mathrm{T}}\mathrm{sig}^{r_4}(S) - k_5 S^{\mathrm{T}}S + \|S\|\tilde{\varepsilon}_1 \\ \leqslant & -k_3 S^{\mathrm{T}}\mathrm{sig}^{r_3}(S) - k_4 S^{\mathrm{T}}\mathrm{sig}^{r_4}(S) \\ \leqslant & -\tau_1 V_4^{\frac{1+r_3}{2}} - \tau_2 V_4^{\frac{1+r_4}{2}}.\end{aligned} \tag{45}$$

Based on (45), we assume that $|\tilde{\varepsilon}_1| \leqslant \chi$, and then the fixed-time stability is held when $\|S\| > \frac{\chi}{k_5}$. Therefore, we conclude that S converges to Δ_{S2}.

Based on Lemma 5 and the above analysis, for the case of $|S_i| < \varepsilon_0$, FNTSMS converges to the region Δ_{S1}. In the case of $|S_i| \geqslant \varepsilon_0$, FNTSMS converges to the region Δ_{S2}. Furthermore, we can conclude from the aforementioned analysis that the sliding variable S converges into the small region Δ_S in the fixed time according to the proposed ANFTSMC law (33).

Step 2. Here, we demonstrate that the attitude errors $\hat{q}_{ei}$ $(i = 1, 2, 3)$ can converge to region Δ_1 in the fixed time, and the angular velocity errors ω_{ei} $(i = 1, 2, 3)$ can converge to region Δ_2 in the fixed time.

Case 1. If $\bar{S}_i = 0$ $(i = 1, 2, 3)$, we obtain that the global position $\hat{q}_i \to 0 \in \Delta_1$ and velocity tracking errors $\omega_{ei} \to 0 \in \Delta_2$ converge to zero in fixed time T_0 according to Lemma 6.

Case 2. If $\bar{S}_i \neq 0$, and $|\hat{q}_{ei}| \leqslant \phi$ $(i = 1, 2, 3)$, it means that $\hat{q}_{ei}$ has converged to a small area $|\hat{q}_{ei}| \leqslant \phi \in \Delta_1$ in the fixed time. Based on (6), we obtain that $\dot{\hat{q}}_{ei} + k_1\mathrm{sig}^{r_1}(\hat{q}_e) + k_2(\iota_1\hat{q}_{ei} + \iota_2\mathrm{sig}^2(\hat{q}_{ei})) = \psi_i$, $\psi_i \in \Delta_S$, $i = 1, 2, 3$. It follows that: $\dot{\hat{q}}_{ei} = |k_1\mathrm{sig}^{r_1}(\hat{q}_{ei})| + k_2|\iota_1\hat{q}_{ei} + \iota_2\mathrm{sig}^2(\hat{q}_{ei})| + |\psi_i| \leqslant \Delta_2$. Therefore, it confirms that $\dot{\omega}_{ei}$ also converges to the region $|\dot{\hat{q}}_{ei}| \leqslant \Delta_2$.

Case 3. If $\bar{S}_i \neq 0$, $|\hat{q}_{ei}| \geqslant \phi$, then

$$\dot{\hat{q}}_{ei} + k_1\mathrm{sig}^{r_1}(\hat{q}_e) + k_2\mathrm{sig}^{r_2}(\hat{q}_{ei}) = \psi_i, \quad \psi_i \in \Delta_S, \tag{46}$$

which is equivalent to the following:

$$\dot{\hat{q}}_{ei} + \left(k_1 - \frac{\psi_i}{\mathrm{sig}^{r_1}(\hat{q}_{ei})}\right)\mathrm{sig}^{r_1}(\hat{q}_{ei}) + k_2\mathrm{sig}^{r_2}(\hat{q}_{ei}) = 0, \tag{47}$$

or

$$\dot{\hat{q}}_{ei} + k_1\mathrm{sig}^{r_1}(\hat{q}_{ei}) + \left(k_2 - \frac{\psi_i}{\mathrm{sig}^{r_2}(\hat{q}_{ei})}\right)\mathrm{sig}^{r_2}(\hat{q}_{ei}) = 0. \tag{48}$$

When $k_1 - \frac{\psi_i}{\mathrm{sig}^{r_1}(\hat{q}_{ei})} > 0$, or $k_2 - \frac{\psi_i}{\mathrm{sig}^{r_2}(\hat{q}_{ei})} > 0$, the above equation has same expression of (10). Applying Lemma 6, it can be concluded that the tracking error $\hat{q}_{ei}$ converges to the region $|\hat{q}_{ei}| \leqslant \Delta_1$ in the fixed time, and $\dot{\hat{q}}_{ei}$ converges to the region $|\dot{\hat{q}}_{ei}| \leqslant \Delta_2$ in the fixed time.

Remark 3. It should be noted that by adjusting the parameters (such as r_3, r_4, k_1, k_2, k_3, k_4), the ranges of convergence regions for S, $\hat{e}$ and ω_e can be derived. Among the parameters, r_3, r_4, k_1, k_2, k_3, and k_4 are crucial and important, as they have considerable effects on achieving the better control performance. The convergence region Δ_S can be adjusted by selecting the parameters r_3, r_4, k_3, and k_4. The convergence regions of the attitude and angular velocity tracking errors can be varied by adjusting the control parameters k_1, k_2, r_1, and r_2. It follows from (37) and (38) that by selecting the larger parameters k_1 and k_2 the convergence region Δ_1 could be decreased and the convergence region Δ_2 could

be increscent. Moreover, it is seen from (39) that the convergence time can be defined in advance by selecting the parameters $r_3,\ r_4,\ k_3$, and k_4. Consequently, from the above rationale, we can conclude that the design parameters have the significant influence on the control performance of the proposed system, while parameters selection requires considering the system requirements comprehensively.

Remark 4. It should be noted that among the controller parameters mentioned in (33), k_3 and k_4 are the crucial and important parameters that have a significant effect on the control performance. It follows from (33) and (39) that the larger are the selected parameters k_3 and k_4, the faster convergence time can be obtained, and at the same time, the larger control energy may be required. Therefore, a certain tradeoff between the convergence time and control energy needs to be achieved in practice.

4 Simulation

In this section, we discuss the control performance of the proposed controller (33)–(35) based on FNTSMS (6) and FxTESO (20) and compare it with that of the controller suggested in [41].

In the simulation, the initial conditions of attitude quaternion and angular velocity are selected as

$$q(0) = [0.3,\ -0.2,\ -0.3,\ 0.8832]^{\mathrm{T}},$$

and

$$\omega(0) = [0,\ 0,\ 0]^{\mathrm{T}}\ \mathrm{rad/s}.$$

The initial desired unit quaternion is formulated as $q_d(0) = [0,\ 0,\ 0,\ 1]^{\mathrm{T}}$, and the desired angular velocity is defined as follows:

$$\omega_d(t) = 0.05\left[\sin\left(\frac{\pi t}{100}\right),\ \sin\left(\frac{2\pi t}{100}\right),\ \sin\left(\frac{3\pi t}{100}\right)\ \right]^{\mathrm{T}}\ \mathrm{rad/s}.$$

Furthermore, the inertia matrix of the spacecraft is selected as follows:

$$J_0 = \begin{bmatrix} 20 & 1.2 & 0.9 \\ 1.2 & 17 & 1.4 \\ 0.9 & 1.4 & 15 \end{bmatrix}\ \mathrm{kg}\cdot\mathrm{m}^2,$$

and

$$\Delta J = \begin{bmatrix} 2 & 0 & 0 \\ 0 & 2 & 0 \\ 0 & 0 & 3 \end{bmatrix}\ \mathrm{kg}\cdot\mathrm{m}^2.$$

The external disturbance is defined as follows: $z(t) = [0.01\sin(0.1t),\ 0.02\sin(0.2t),\ 0.03\sin(0.3t)]^{\mathrm{T}}$.

4.1 The performance of the proposed controller

In this subsection, the efficiency of the proposed controller (33) based on FNTSMS (6) and FxTESO (20) is illustrated. The observer gains corresponding to FxTESO (20) are the following: $\alpha_1 = 3$; $\beta_1 = 15$; $\alpha_2 = 1.5$; $\beta_2 = 7.5$; $o_1 = 0.9$; $\theta_1 = 1.01$; when $|E_{1i}| > 0.01$, and $\Lambda = 0$. The parameters associated with FNTSMS (6) are defined as: $k_1 = 2$; $k_2 = 0.2$; $r_1 = \frac{11}{5}$; and $r_2 = \frac{11}{19}$. The controller parameters are set as: $k_3 = 3.3$; $k_4 = 20$; $k_5 = 0.001$; $r_3 = \frac{11}{5}$; and $r_4 = \frac{11}{19}$.

Figure 2 represents the trajectories of the disturbances and observers exhibiting that FxTESO (20) has the acceptable performance in terms of estimating the total uncertainty G.

Figure 3 illustrates the trajectories of the sliding surface (6). It can be seen that the system trajectory is driven onto the sliding surface and finally converges to a small region near the origin.

The input control signal is represented in Figure 4, which demonstrates that the undesired chattering can be reduced efficiently by applying estimation and compensation through FxTESO (20). Furthermore, Figure 5 depicts the attitude tracking errors q_{ei} $(i = 1, 2, 3, 4)$, and Figure 6 outlines the angular velocity tracking errors w_{ei} $(i = 1, 2, 3)$. These figures show that the attitude and angular velocity tracking errors converge to small region in finite time, respectively.

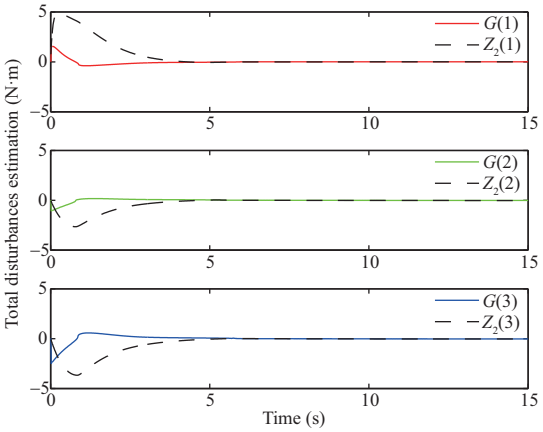

Figure 2 (Color online) The response of the estimated uncertainties corresponding to FxTESO combined with FNTSMS.

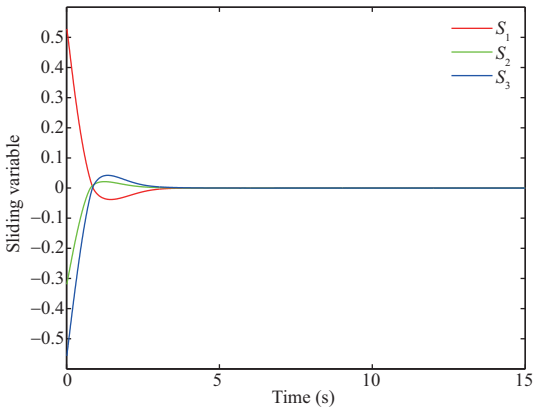

Figure 3 (Color online) Sliding mode surface.

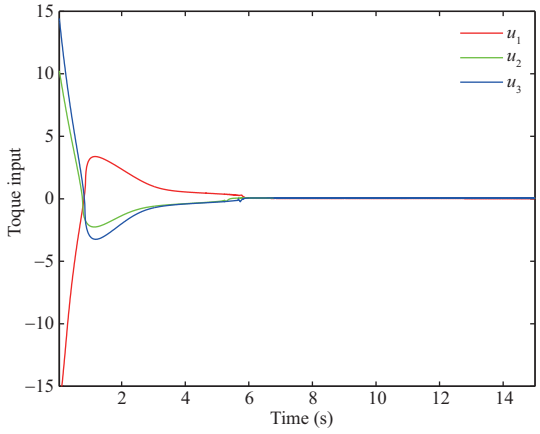

Figure 4 (Color online) The input control.

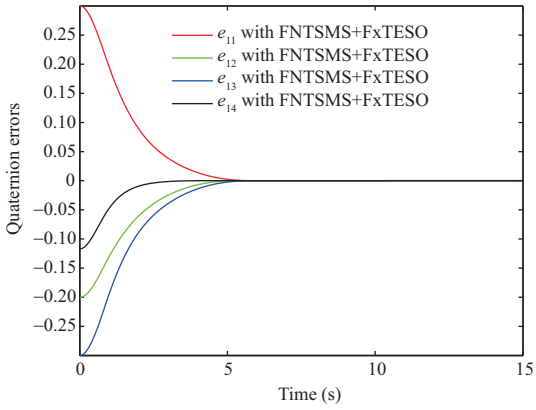

Figure 5 (Color online) Attitude tracking errors corresponding to the FNTSMC law.

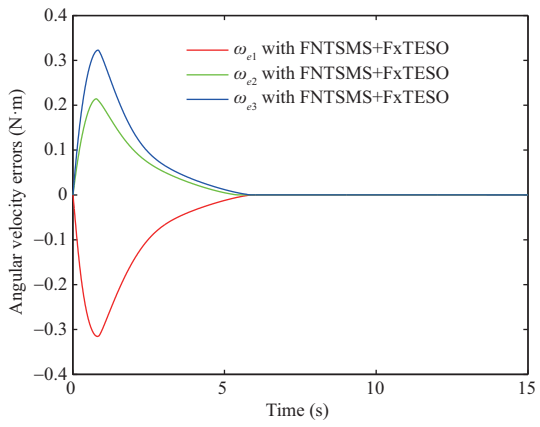

Figure 6 (Color online) Angular velocity tracking errors corresponding to the FNTSMC law.

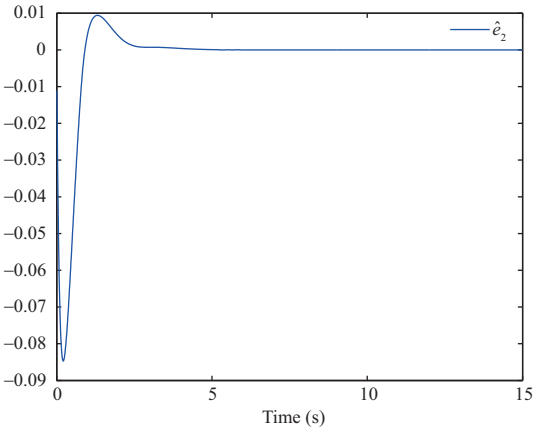

Figure 7 (Color online) Adaption law of observation.

The adaptive parameter $\hat{e}_2$ is represented in Figure 7, which confirms that the adaptive law (35) has the appropriate performance on the observation error.

Based on the above simulations results, we conclude that a preferable control performance in terms of

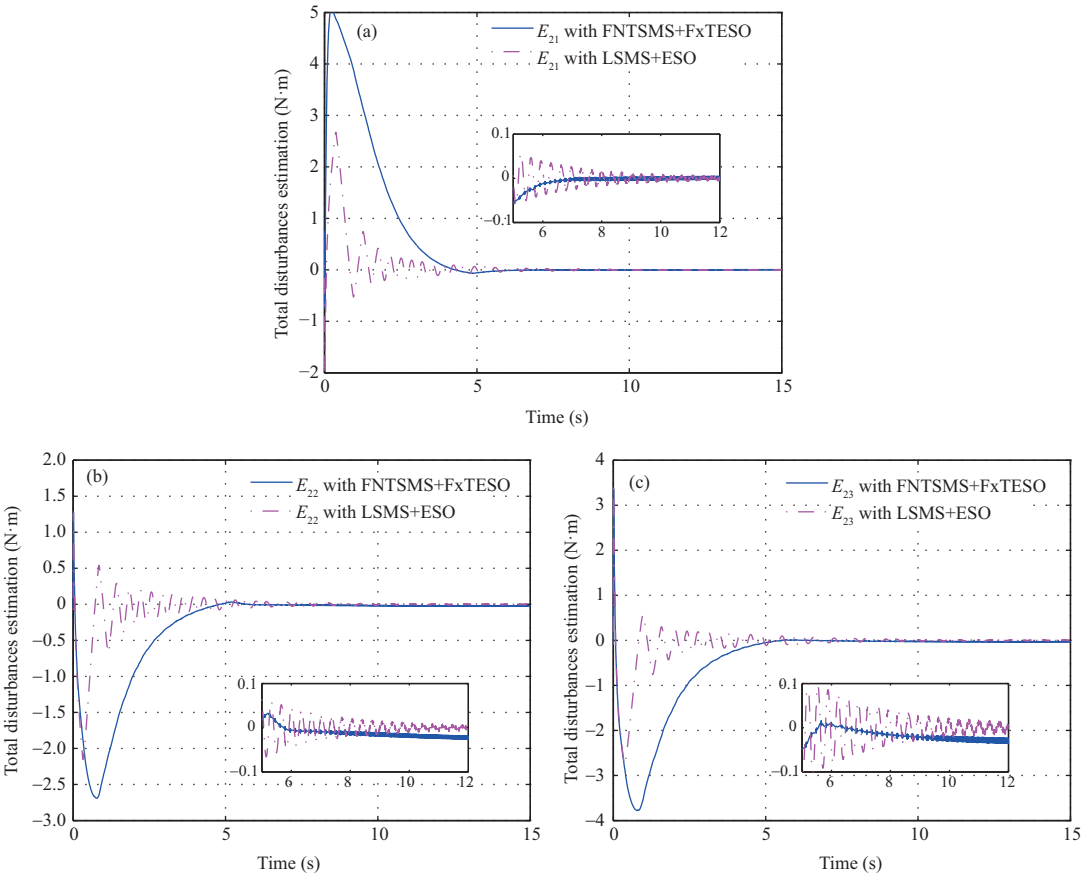

Figure 8 (Color online) The comparison of observation errors under controller (33) and controller in [41]. The response of (a) E_{21}; (b) E_{22}; (c) E_{23}.

attitude tracking can be achieved by the controller defined according to (33) based on FxTESO (20) and FNTSMS (6) in the presence of model uncertainties and external disturbances, simultaneously.

4.2 Comparison of the two controllers

To further confirm the superiority of the performance in terms of higher precision, faster convergence rate, and better disturbance rejection of the proposed controller (33) based on FxTESO (20) and FNTSMS (6), we compare it with the controller developed in [41]. To perform a fair comparison, the same parameters as for the control method in [41] are set as follows: $\alpha_2 = 1.5$; $\beta_2 = 7.5$; and $k_1 = 2$. The comparison results are presented in Figures 8–12. Figure 8 demonstrates the comparison results corresponding to the observation errors. It is observed that the proposed FxTESO (20) provides a faster convergence rate and higher convergence accuracy compared with those of [41]. The system trajectory is driven onto the sliding surface and finally converges to the origin, which is illustrated in Figure 9. It is found that compared with the linear sliding mode in [41], the convergence time of the proposed FNTSMS is faster, while the chattering can be reduced efficiently. The input control signals are depicted in Figure 10, indicating that the undesired chattering can be reduced successfully by applying estimation and compensation via FxTESO, compared with the controller suggested in [41]. Figures 11 and 12 represent the comparison results corresponding to the attitude tracking errors $\hat{e}_i$ $(i = 1, 2, 3)$ and angular velocity tracking errors ω_{ei} $(i = 1, 2, 3)$ obtained for the proposed controller (33) and the one suggested in [41]. It is observed that the controller (33) provides a faster and more accurate response, as well as better chattering suppression compared with those obtained for [41].

From the results presented in Figures 8–12, we conclude that the FNTSMC controller (33)–(35) based on FNTSMS (6) and FxTESO (20) allows achieving better control performance in terms of the faster convergence rate, better disturbance rejection, stronger robustness, and higher precision compared with the control law suggested in [41].

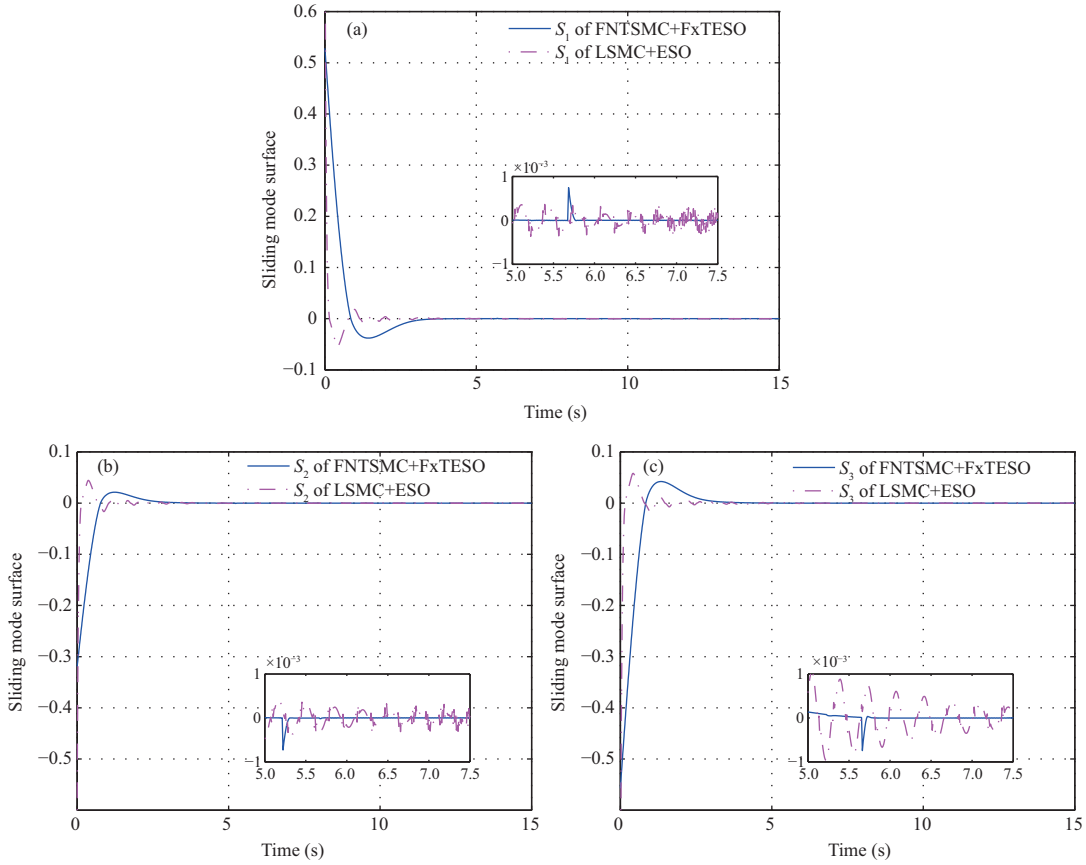

Figure 9 (Color online) The comparison of S corresponding to the controller (33) and controller by [41]. The response of (a) S_1; (b) S_2; (c) S_3.

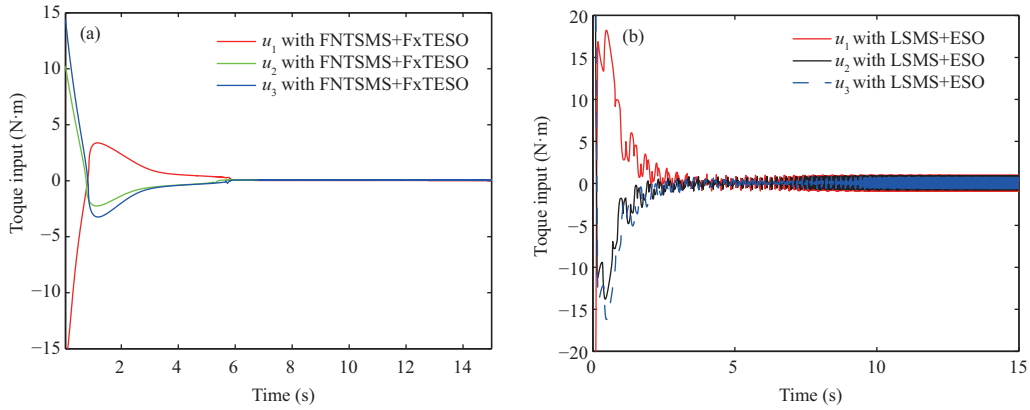

Figure 10 (Color online) (a) The u corresponding to the controller (33); (b) the u corresponding to the controller by [41].

5 Conclusion

In the present paper, we consider the fixed-time attitude tracking control problem for spacecraft affected by model uncertainties and external disturbances. The FNTSMC controller has been developed on the basis of FNTSMS, FxTESO, and the adaptive law. The differentiable uncertainties have been estimated and compensated by using the proposed FxTESO, which considers the actuator inertia uncertainties and external disturbances as extended state variables. Moreover, the FNTSMC scheme has been designed to ensure the closed-loop system stability by considering the Lyapunov theory. It has been proved that the proposed FNTSMC scheme makes the tracking error converge to a small neighborhood of zero in the fixed time. The efficiency of the proposed control law has been verified by conducting theoretical analysis

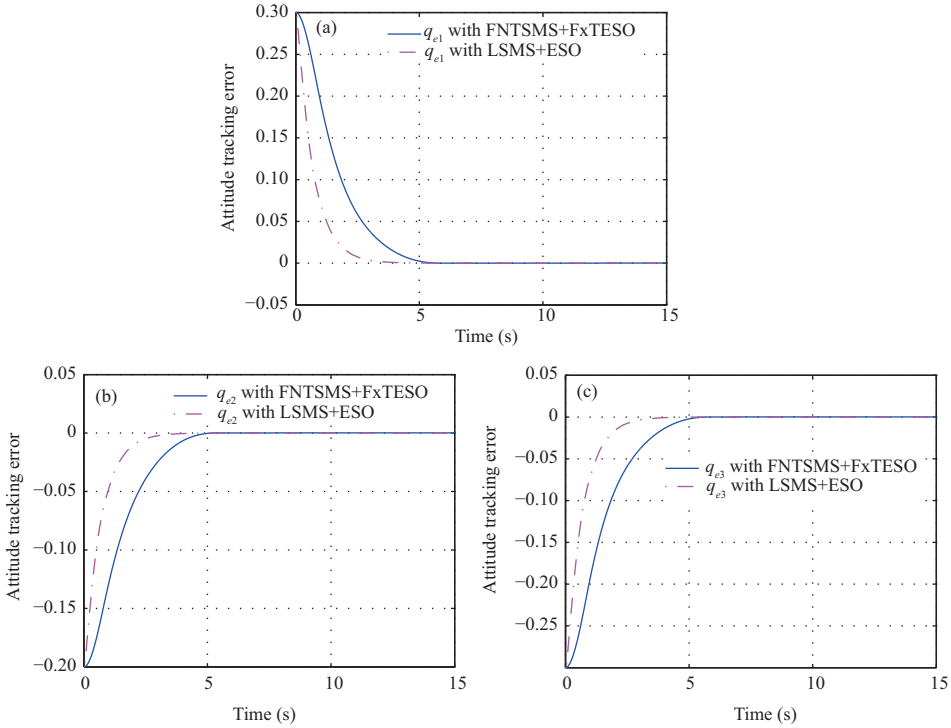

Figure 11 (Color online) The comparison of the attitude tracking errors corresponding to the controller (33) and controller by [41]. The response of (a) q_{e1}; (b) q_{e2}; (c) q_{e3}.

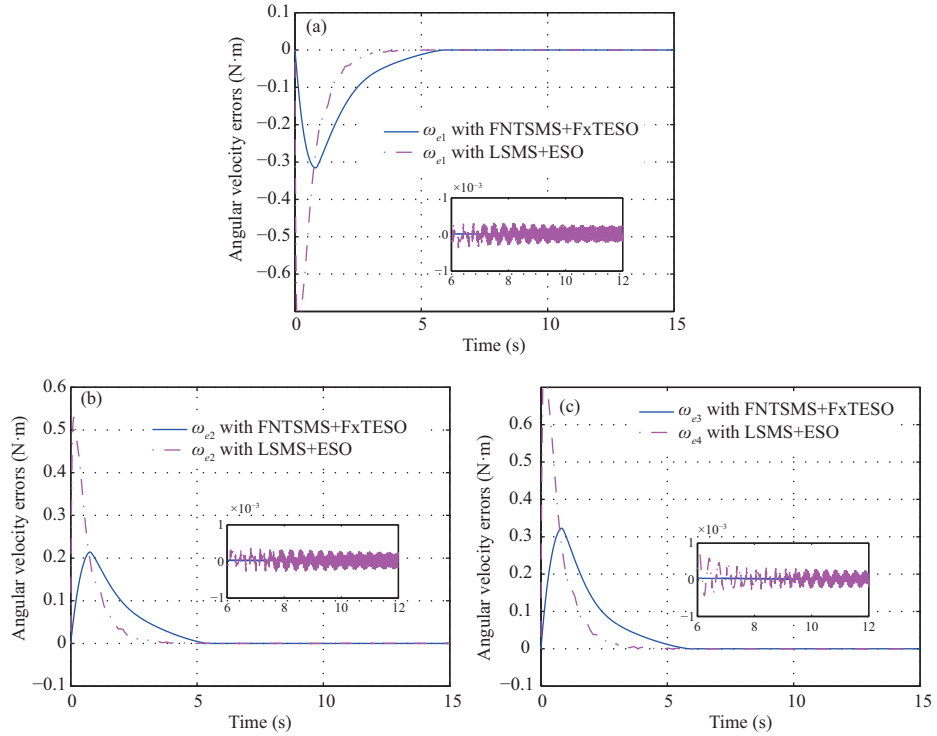

Figure 12 (Color online) The comparison of the angular tracking errors corresponding to the controller (33) and the one by [41]. The response of (a) ω_{e1}; (b) ω_{e2}; (c) ω_{e3}.

and simulation experiments.

Acknowledgements This work was supported in part by National Natural Science Foundation of China (Grant No. 61720106010), in part by Science and Technology on Space Intelligent Control Laboratory (Grant No. KGJZDSYS-2018-05).

References

1 Du H B, Li S H, Qian C J. Finite-time attitude tracking control of spacecraft with application to attitude synchronization. IEEE Trans Autom Control, 2011, 56: 2711–2717

2 Xie Y C, Zhang H, Hu J, et al. Automatic control system design of Shenzhou spacecraft for rendezvous and docking (in Chinese). Sci Sin Tech, 2014, 44: 12–19

3 Dong H Y, Hu Q L, Ma G F. Dual-quaternion based fault-tolerant control for spacecraft formation flying with finite-time convergence. ISA Trans, 2016, 61: 87–94

4 Buzzoni A, Altavilla G, Galleti S. Optical tracking of deep-space spacecraft in Halo L2 orbits and beyond: the Gaia mission as a pilot case. Adv Space Res, 2016, 57: 1515–1527

5 Xia K W, Huo W. Adaptive control for spacecraft rendezvous subject to actuator faults and saturations. ISA Trans, 2018, 80: 176–186

6 Cui B, Xia Y Q, Liu K, et al. Velocity-observer-based distributed finite-time attitude tracking control for multiple uncertain rigid spacecraft. IEEE Trans Ind Inf, 2020, 16: 2509–2519

7 Hu Q L, Xiao B, Friswell M I. Robust fault-tolerant control for spacecraft attitude stabilisation subject to input saturation. IET Control Theory Appl, 2011, 5: 271–282

8 Huo X, Hu Q L, Xiao B. Finite-time fault tolerant attitude stabilization control for rigid spacecraft. ISA Trans, 2014, 53: 241–250

9 Ma G F, Li B, Yu Y B. Observer-based fault diagnosis incorporating adaptive sliding mode control for spacecraft attitude stabilization. In: Proceedings of the 34th Chinese Control Conference (CCC), 2015. 6224–6229

10 Jin E, Sun Z W. Robust controllers design with finite time convergence for rigid spacecraft attitude tracking control. Aerosp Sci Technol, 2008, 12: 324–330

11 Zou A M, Kumar K D, Hou Z G, et al. Finite-time attitude tracking control for spacecraft using terminal sliding mode and chebyshev neural network. IEEE Trans Syst Man Cybern B, 2011, 41: 950–963

12 Zou A M. Finite-time output feedback attitude tracking control for rigid spacecraft. IEEE Trans Control Syst Technol, 2014, 22: 338–345

13 Yoo D, Yau S S T, Gao Z Q. Optimal fast tracking observer bandwidth of the linear extended state observer. Int J Control, 2007, 80: 102–111

14 Yang J, Cui H Y, Li S H, et al. Optimized active disturbance rejection control for DC-DC buck converters with uncertainties using a reduced-order GPI observer. IEEE Trans Circ Syst I, 2018, 65: 832–841

15 Lu K F, Xia Y Q, Zhu Z, et al. Sliding mode attitude tracking of rigid spacecraft with disturbances. J Franklin Inst, 2012, 349: 413–440

16 Yang H J, You X, Xia Y Q, et al. Adaptive control for attitude synchronisation of spacecraft formation via extended state observer. IET Control Theory Appl, 2014, 18: 2171–2185

17 Hu Q L, Shao X D, Chen W H. Robust fault-tolerant tracking control for spacecraft proximity operations using time-varying sliding mode. IEEE Trans Aerosp Electron Syst, 2018, 54: 2–17

18 Yang J, Li T, Liu C J, et al. Nonlinearity estimator-based control of a class of uncertain nonlinear systems. IEEE Trans Autom Control, 2020, 65: 2230–2236

19 Venkataraman S T, Gulati S. Terminal sliding modes: a new approach to nonlinear control synthesis, In: Proceedings of International Conference on Advanced Robotics Robots in Unstructured Environments, 1991. 443–448

20 Feng Y, Yu X H, Man Z H. Non-singular terminal sliding mode control of rigid manipulators. Automatica, 2002, 38: 2159–2167

21 Shen G H, Xia Y Q, Zhang J H, et al. Finite-time trajectory tracking control for entry guidance. Int J Robust Nonlinear Control, 2018, 28: 5895–5914

22 Zhao L, Jia Y M. Finite-time attitude tracking control for a rigid spacecraft using time-varying terminal sliding mode techniques. Int J Control, 2015, 88: 1150–1162

23 Hu Q L, Niu G L. Attitude output feedback control for rigid spacecraft with finite-time convergence. ISA Trans, 2017, 70: 173–186

24 Cao L, Qiao D, Chen X Q. Laplace ι_1 Huber based cubature Kalman filter for attitude estimation of small satellite. Acta Astronaut, 2018, 148: 48–56

25 Xia Y Q, Zhu Z, Fu M Y. Back-stepping sliding mode control for missile systems based on an extended state observer. IET Control Theory Appl, 2011, 5: 93–102

26 Talole S E, Kolhe J P, Phadke S B. Extended-state-observer-based control of flexible-joint system with experimental validation. IEEE Trans Ind Electron, 2010, 57: 1411–1419

27 Zhou C B, Zhou D. Robust dynamic surface sliding mode control for attitude tracking of flexible spacecraft with an extended state observer. Proc Inst Mech Eng Part G-J Aerosp Eng, 2017, 231: 533–547

28 Yang J, Shi X P, Li L, et al. Nonlinear observer based time delay fault-tolerant attitude control for flexible spacecraft during orbit maneuver. In: Proceeding of the 27th Chinese Control and Decision Conference (CCDC), 2015. 50–57

29 Zhong C X, Guo Y, Yu Z, et al. Finite-time attitude control for flexible spacecraft with unknown bounded disturbance. Trans Inst Meas Control, 2016, 38: 240–249

30 Li B, Hu Q L, Yu Y B, et al. Observer-based fault-tolerant attitude control for rigid spacecraft. IEEE Trans Aerosp Electron Syst, 2017, 53: 2572–2582

31 Pukdeboon C. Extended state observer-based third-order sliding mode finite-time attitude tracking controller for rigid spacecraft. Sci China Inf Sci, 2019, 62: 012206

32 Zhang L, Wei C Z, Wu R, et al. Fixed-time extended state observer based non-singular fast terminal sliding mode control for a VTVL reusable launch vehicle. Aerosp Sci Tech, 2018, 82: 70–79

33 Hardy G, Littlewood J, Polya G. Inequalities. Cambridge: Cambridge University Press, 1952

34 Huang X Q, Lin W, Yang B. Global finite-time stabilization of a class of uncertain nonlinear systems. Automatica, 2005, 41: 881–888

35 Kollatc L. Problems on Eigenvalues. Moscow: Science, 1968

36 Bhat S P, Bernstein D S. Geometric homogeneity with applications to finite-time stability. Math Control Signal Syst, 2005, 17: 101–127

37 Yu S H, Yu X H, Shirinzadeh B, et al. Continuous finite-time control for robotic manipulators with terminal sliding mode. Automatica, 2005, 41: 1957–1964

38 Polyakov A. Nonlinear feedback design for fixed-time stabilization of linear control systems. IEEE Trans Autom Control, 2012, 57: 2106–2110

39 Khalil H. Nonlinear Systems. Englewood Cliffs: Prentice-Hall Press, 2002

40 Basin M, Yu P, Shtessel Y. Finite- and fixed-time differentiators utilising HOSM techniques. IET Control Theory Appl, 2017, 22: 1144–1152

41 Lu K F, Xia Y Q, Fu M Y. Controller design for rigid spacecraft attitude tracking with actuator saturation. Inf Sci, 2013, 220: 343–366

42 Basin M V, Yu P, Shtessel Y B. Hypersonic missile adaptive sliding mode control using finite- and fixed-time observers. IEEE Trans Ind Electron, 2018, 65: 930–941